



In Vitro Evaluation of Cytotoxicity and Antimicrobial Activity of Green Synthesized Silver Nanoparticles Based on Their Particle Size and Stability



Shimaa Farag hamieda* and Mona Saied

Microwave Physics and Dielectrics Department, National Research Centre, Giza, Egypt.

Abstract

In the present study, we report the simple, inexpensive, and eco-friendly synthesis of silver nanoparticles (AgNPs) to assess their potential in biomedical applications based on their particle size and stability. Therefore, two different AgNP samples were prepared using sunflower seed cake (SSC) and pomegranate peel (PP) aqueous extract. Different spectroscopic techniques were used to characterize the synthesized SSC-AgNPs and PP-AgNPs. Ultraviolet-Visible (UV) Spectroscopy showed the characteristic peak around 450 nm which is characteristic to AgNPs. TEM analysis depicted the spherical morphology of SSC-AgNPs and PP-AgNPs with 4.46–10.16 nm and 14.11–47.77 nm respectively. Dynamic light scattering (DLS) analysis showed that SSC-AgNPs and PP-AgNPs showed negative zeta potential value -9.79 and -24.22 mV respectively. The results of the XRD indicated that SSC-AgNPs and PP-AgNPs were in face centered cubic structure. Also, the results of Fourier transform infrared (FTIR) research showed that the SSC and PP extract contained proteins and polyphenols. Also, cytotoxicity studies using hemolytic and normal cell viability assays, as well as, MCF7 anticancer activity and the inhibition activity against three microbial strains of both AgNPs were investigated. The results showed that SSC-AgNPs and PP-AgNP were biologically compatible at concentration 2000 µg/mL and 250 µg/mL while reduced cancer cell viability at concentration 1878 µg/mL and 1140 µg/mL respectively. Therefore, SSC-AgNPs are better suited for biomedical applications than PP-AgNPs. It could be concluded that biosynthesis formation of AgNPs with different size and stability possess different impact on cytotoxicity and biological activity.

Keywords: Spectroscopy; Cytotoxicity; Antibacterial and Anticancer

1. Introduction

Several physical and chemical methods such as laser radiation, ultrasound irradiation and sol gel have been developed for synthesis of AgNPs. However, such methods are costly, and some of the chemicals used to synthesize AgNPs have the potential to pollute the environment. Thus, the need for an ecologically friendly AgNP synthesis is increasing. A variety of biological materials have been used for the synthesis of AgNPs, such as milk and microorganisms. [1]. But some of problems, like mass microorganism cultivation, had decreased the application. Hence, plant extract, oil cake, and inexpensive, readily available agro-industrial waste were utilized in "green synthesis," a process that produces AgNPs at a low cost and with minimal preparation. The biomolecules found in oil cake have the ability to reduce the silver ions. [2,3]. Govarathanan et al. [3] reported the environmentally friendly, sustainable synthesis of silver nanoparticles using coconut oil cake extract. Also, the medicinal properties of Pomegranate peel have been attributed to the presence of various phytochemical compounds including flavonoids, polyphenols, proteins and vitamins [4]. These biomolecules act as stabilizing agents for the nanoparticles. [5].

The synthesis of nanoparticles is influenced by various factors such as the type of plant used, the organic compounds present in the crude seed extract, the temperature, the concentration of silver nitrate, and even the pigments in the leaf extract [5]. Several factors, such as the size and shape of the nanoparticles or the type of capping material covering the particle surface, influence the physical, chemical, and biological characteristics of AgNPs. [6]. AgNPs have the potential to enter the bloodstream via the dermal junction and medicine, where they can then interact with plasma proteins and blood cells to trigger pathophysiologic processes within the circulatory system. Furthermore, since silver is an essential element of medical devices,

*Corresponding author e-mail: shimaafarag1982@yahoo.com; (Shimaa Farag hamieda).

Received date 14 October 2024; revised date 31 October 2024; accepted date 10 November 2024

DOI: 10.21608/ejchem.2024.328372.10631

©2025 National Information and Documentation Center (NIDOC)

research on how it interacts with blood and blood compatibility is necessary to exploit the potential importance of AgNPs in medicine and the development of medical devices. [7].

AgNPs have been employed in numerous physical, chemical, biological, and medicinal domains to prevent bacterial infections. Bacterial cells' cell walls and membranes are damaged by silver nanoparticles which alters their morphology [8]. Silver nanoparticles are efficient against Gram-positive and Gram-negative bacteria, according to numerous studies.[9] All of these factors play a vital role the crucial features of nanoparticles are their size, which must fall within the range of 1-100 nm [10] Antibacterial activity is significantly influenced by the nanoparticles' size. The results of different investigations showed that the ability of a nanoparticle to enter bacteria increases with decreasing nanoparticle size. [11,12]. There is still some debate as to why AgNPs have an antibacterial impact on bacteria.

Even though a lot of research on the synthesis of nanoparticles has been published, none of them have looked at how the produced particles aggregate and how that affects biological activity. Indeed, biological activity in living systems can be directly impacted by the colloidal stability of nanoparticles. [6] Described synthesis techniques for the creation of green nanomaterials and demonstrated how the different green materials used for metal ion reduction and stabilization play an essential role in determining the biological activity of the resulting green nanoparticles. Results on the agglomeration of bare AgNPs under environmentally relevant conditions were presented by Elzey and Grassian. However, their studies did not focus on the effects of nanoparticle aggregation on toxicity. It is well-known that nanomaterials can interact with a variety of living organisms' biomolecules. [13]. There is a lack of information in the scientific literature concerning AgNP aggregation behavior, and especially its relation to cytotoxicity and the biological activity of AgNPs [6]. Therefore, in this paper two different AgNP samples were synthesized using sunflower seed cake and pomegranate peel extract, additional structural and morphological analysis of the synthesized Ag NPs was carried out using a variety of techniques, such as transmission electron microscopy and an X-ray diffractometer, Dynamic light scattering (DLS), UV-Vis spectrophotometry and Fourier Transform Infrared Spectroscopy (FTIR).

Our aim was to investigate the effects of particle size and stability on the aggregation behavior of these particles in order to evaluate its impact on cytotoxicity by using hemolytic assay and normal cell viability, as well as antimicrobial and anticancer activity.

2. Materials processing and Experimental techniques

2.1. Materials Processing

2.1.1. Preparation of SSC and PP extracts

The sun flower seed cake SSC and pomegranate peel PP were collected from local super market. These samples then washed with water and dried at 50C°. The SSC was grinded at oils mills of Ismailia region in Egypt, while PP was grinded at mill of national research center. Ten grams of each sample were dissolved in one hundred milliliters of deionized boiling water, and then filtered through filter paper No. 1. The sun flower seed cake and pomegranate peel used in this research are wastes and present in large amount. This research involving species not at risk of extinction that complies with relevant institutional, national, and international guidelines and legislation.

Synthesis of AgNPs

SSC and PP aqueous extracts were used to synthesize AgNPs. The Ag NPs were produced by adding 25 ml of each extract to 225 ml of 1mM AgNO₃ [2].

2.2. Experimental techniques

2.2.1. UV-Vis spectroscopy

Absorption spectrum was taken at 350–700 nm with a UV-vis-spectrophotometer (JASCO,V-360 spectrophotometer) to check NPs formation from the two extracts.

2.2.2. Transmission Electron Microscope (TEM)

To determine the size and shape of the AgNPs, samples were examined using TEM. A high resolution transmission electron microscope was used to examine the electron diffraction patterns and particle size (JEOL JX 1230 -HRTEM).

2.2.3. Dynamic light scattering (DLS)

Zeta potential data of the samples were obtained by DLS technique. Zeta Sizer Nano ZS (Particle Sizing Systems, Inc. Santa Barbara, Calif., USA). Zeta Sizer, a software program from the same manufacturer, was used to process the data acquired in triplicate.

2.2.4. Fourier Transform Infrared Spectroscopy (FTIR)

A Fourier transform infrared spectrometer was used to obtain infrared spectra (JASCO FT/IR 300 E (Tokyo, Japan)) in KBr pellets at a resolution of 4 cm⁻¹.

2.2.5. X-ray diffraction pattern (XRD)

XRD was performed using (Empyrean Panalytical X-ray diffractometer equipped with CuK radiation). The scanning was done in the region of 2 θ =30–80°. The Scherrer equation was used to determine the crystallite size (nm). $D = K\lambda/\beta 0.5\cos\theta$. where λ wavelength (1.54 Å), d indicates crystallite size (nm), K indicates Scherrer constant (0.94), $\beta 0.5$ indicates full width at half maximum length, and θ indicates Bragg's angle in radian.

2.2.6. Haemolytic assay

The synthesized SSC-AgNPs and PP-AgNPs; were submitted to *in vitro* studies for the preliminary evaluation of hemocompatibility. Using a hemolytic assay as mentioned by [7]. Three male albino rats weighing 250 –300 g will be used for the present study. Animals were obtained from the National Research Center (Giza, Egypt). Three milliliters of rat blood were drawn into a sodium citrate tube. Different concentrations (20000, 10000, 5000, 2000, 500 and 250 µg/mL) of Ag NPs were took in test tubes then added 200 µL of citrated blood to each test tube, and the final volume maintained at 2 mL. After one hour of incubation at 37°C, these were centrifuged for ten minutes at 3000 rpm, and the absorbance of the supernatant was measured at 540 nm, a blood/water mixture was used as the positive reference, and a blood/saline mixture served as the negative control. The percentage of hemolysis was calculated using the following equation:

$$\text{Hemolysis \%} = [(A_{\text{sample}} - A_{\text{control}}) / (A_{\text{positive}} - A_{\text{control}})] \times 100$$

Where A is the absorbance

Anesthetic procedures and handling with animals complied with the ethical guidelines of Medical Ethical Committee of the National Research Centre in Egypt.

2.2.7. Cytotoxic effect on human normal fibroblast (BJI) and breast cancer (MCF7) cell line:

In this study, we did not employ any primary cell lines. The assessment of cell viability was conducted through the reduction of yellow MTT (3-(4,5-dimethylthiazol-2-yl)-2,5-diphenyl tetrazolium bromide) to purple formazan in a mitochondrial-dependent manner. [14]. Using a Laminar flow cabinet biosafety class II (Baker, SG403INT, Sanford, ME, USA). Cells were suspended in 1% antibiotic–antimycotic combination (10,000 U/ml Potassium Penicillin, 10,000 IU/ml Streptomycin Sulphate, and 25 IU/ml Amphotericin B) and 1% L-glutamine at 37°C under 5% CO₂. (for HePG2-MCF7 and HCT116—DMEM for A549 and PC3). The cells were cultivated in a batch for ten days and then seeded into 96-well microtiter plastic plates with fresh complete growth medium at a concentration of 10⁴–10⁵ cells/well. The plates were kept at 37°C for 24 hours with 5% CO₂ using a water-jacketed carbon dioxide incubator (Sheldon, TC2323, Cornelius, OR, USA). After aspirating the media and adding fresh medium without serum, the cells were incubated either in the absence of the sample (negative control) or with varying doses of it, resulting in a final concentration of (8000, 4000, 2000, 1000, 500, 250, 125, and 62.5 µg/mL). Each well received 40 µL MTT salt (2.5 mg/mL) after the medium had been aspirated after 48 hours of incubation. The wells were then left to incubate for an additional four hours at 37 °C with 5% CO₂. A natural cytotoxic substance known to be 100% deadly under identical conditions was employed as a positive control, containing 100 µg/mL [15]. A microplate multi-well reader (Bio-Rad Laboratories Inc., model 3350, Hercules, California, USA) was then used to measure the absorbance at 595 nm using a reference wavelength of 620 nm. By utilising the independent t-test in the SPSS 11 software, a statistical significance was examined between the samples and the negative control (cells containing a vehicle).

Cytotoxic activity test was conducted and determined by the Bioassay-Cell Culture Laboratory, NRC, Giza, Egypt. The experiment employed two distinct cell lines: MCF7, a well-established human breast adenocarcinoma model (ATCC® HTB-22™), and hTERT BJ1, a normal human skin fibroblast cell line immortalized by hTERT telomerase (ATCC® CRL-4000™) hTERT BJ1. These cell lines were generously provided by Prof. Stig Linder of the Karolinska Institute (Sweden).

2.2.8 Antimicrobial study

According to a previous study, qualitative evaluations were executed in nutrient agar plates [16]. The inoculation of all microorganisms was prepared from fresh overnight broth cultures using Nutrient Broth medium (NB) incubated at 37°C [17]. The inoculum size was prepared and adjusted to 0.5 McFarland standard (1.5 × 10⁸ CFU/ mL) approximately [18]. Each plate containing 20.0 mL of the sterile nutrient agar medium (NA) inoculated 25.0 µL of both bacterial and fungal suspensions separately, by using 1.0 cm cork borer applying Well Diffusion Method. After the media cooled and solidified, 100.0 µL of the prepared samples were separately applied on 0.9 cm well of that inoculated agar plates prepared previously [19,20]. These inoculated plates were placed in the refrigerator for one hour followed by incubation at 37°C for 24 hours. The inhibition zones were measured in mm [19].

Using Nutrient Broth medium, the sample was passed to another test for determination of minimum inhibitory concentration value (MIC) applying micro dilution broth method. [21 and 22].

The change in viability % was calculated according to the formula:

$$((\text{Reading of extract} / \text{Reading of negative control}) - 1) \times 100 \quad \dots\dots\dots (2)$$

Ethical approval

All the methods were carried out in accordance with relevant institutional guidelines and regulations.

3. Results and discussion.

3.1. UV-Vis spectroscopy

The reaction mixture containing 1 mM of AgNO₃ and the extract was turned to dark brown color (AgNPs). The dark brown colour indicated the biosynthesis of AgNPs [23]. Following the visual observation of the synthesis of AgNPs (SSC and PP), UV-Vis analysis of this brownish solution also shows the AgNPs' formation, with an average absorption peak located at 450 nm. SSC-AgNPs and PP-AgNPs had absorption band at maximum of (448 and 460) nm respectively as shown in Figure (1a). Also, it showed an increase in peak intensity of PP-AgNPs compared to SSC-AgNPs, it could possibly be attributed to the increased concentration of the formed PP-NPs. These findings might be consistent with other studies from literature [23] correlating the metal nanoparticle size to the wavelength of the resonant frequency and [1] who demonstrated how an increase in plant extract concentration led to an increase in the size and concentration of the prepared AgNPs. Moreover, the sample containing only extract or even AgNO₃ does not have these absorption peaks as seen in Figure (1b).

3.2. Fourier Transform Infrared Spectroscopy (FTIR)

The IR absorption spectra of SSC and PP pure extracts in Figure 1 (c&d) shows the presence of various functional groups, such as those found in fats, biomolecules, hydrogen nitride, and carbon monoxide. Additionally, surface chemistry of the nanoparticles was investigated using IR spectroscopy. FT-IR analysis revealed the strong bands at 3281, 2931, 1629, 1402 and 1034 cm^{-1} for SSC extract. While PP extract showed strong band at 3279, 2929, 1717, 1338 and 1026 cm^{-1} . Indeed, during the growth stage, biomolecules, especially proteins and polyphenols, did not only assist in the reduction of silver ions but also surrounded and prevented them from agglomeration. In our study we observed that The FTIR spectra of PP-AgNPs were very similar to those of PP extracts, and there were no excess peaks in the range of 500–550 cm^{-1} , according to the metal ions of silver. This demonstrated that all ions of silver participated in the formation of the nanoparticles. On the other hand, the synthesized SSC-AgNPs exhibited the same IR spectra as the SSC aqueous extract but, a great reduction in the peak was seen at 1027 cm^{-1} which is related to the carboxylic group of polypeptides and proteins [24]. Furthermore, peaks observed in the extract at 3281 cm^{-1} completely vanished in the SSC-AgNPs, indicating the participation of protein groups, alcohols, and polyphenols in the catalytic reduction of AgNO_3 to AgNPs. [2]. This result is in agreement with IR spectrum of the synthesized silver nanoparticles from aqueous extracts of COC [3]. The results clearly demonstrated the presence large amounts of residual extract components capping agents on the surface of PP-AgNPs compared to SSC-AgNPs. This could be explained by the PP extract having more reducing agents than SSC extract.

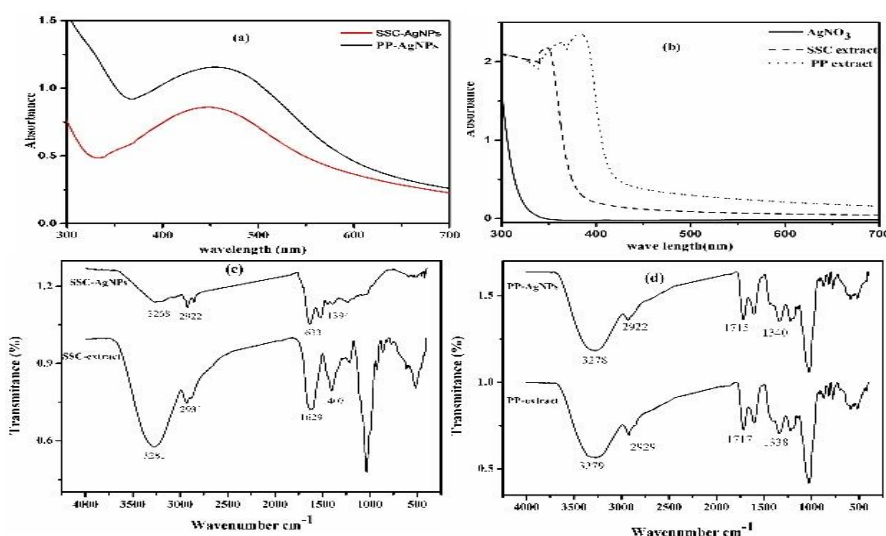


Fig.1: UV-Vis spectra of (SSC and PP) AgNPs (a) and Ag NO_3 , SSC and PP extracts (b). FT-IR spectra of SSC (extract & AgNPs) (c) and PP (extract & AgNPs) (d).

3.3. Transmission Electron Microscope (TEM)

TEM techniques were used to characterize the size and shape of the synthesized AgNPs. TEM images of the synthesized SSC-AgNPs and PP-AgNPs are shown in Figure 2 (a & b) respectively. TEM analysis revealed that SSC-AgNPs and PP-AgNPs are spherical in shape with sizes ranging between (4.46–10.16) and (14.11–47.77) nm respectively. TEM results are consistent with previous report [2], who revealed that the synthesized AgNPs using sesame oil cake had a spherical shape with diameters ranging from (6.6 to 14.8) nm. Furthermore, it is also possible to confirm visually that SSC-AgNPs had smaller diameter when compared to PP-AgNPs.

3.4. X-ray diffraction pattern

The XRD analysis of SSC-AgNPs and PP-AgNPs was carried out to determine its crystalline nature. XRD pattern of SSC-AgNPs and PP-AgNPs in Figure (2c) showed 3 characteristic diffraction peaks at $2\theta = 38.007^\circ$, 44.143° , 64.360° & 77.296° and 38.020° , 44.192° , 64.255° & 77.159° respectively which can be indexed to 111, 200, 202 and 311. The peaks demonstrated the face-centered cube structure of the resulting nanoparticles.

These peaks corroborate with the standard Ag (JCPDS 96-901-3048). The findings are consistent with several studies reported the cubic nature of green synthesized AgNPs [1,3]. Furthermore, the Scherrer equation was used to determine the average crystal sizes of PP-AgNPs and SSC-AgNPs and were found to be around 20.3 and 175.5 nm respectively. The relative peaks positions at the 2θ angles in the XRD pattern of the biosynthesized AgNPs of the two extracts indicating the formation of nanoparticles having equivalent geometry. The sharpness and increase in intensity of spectra means that AgNPs extracted by PP had more crystallinity than AgNPs extracted by SSC [24]. In addition, some extra, unidentified peaks were observed at the

vicinity of the characteristic peaks of silver nanoparticles. These peaks could be due to proteins or other bioorganic compounds of the extracts.

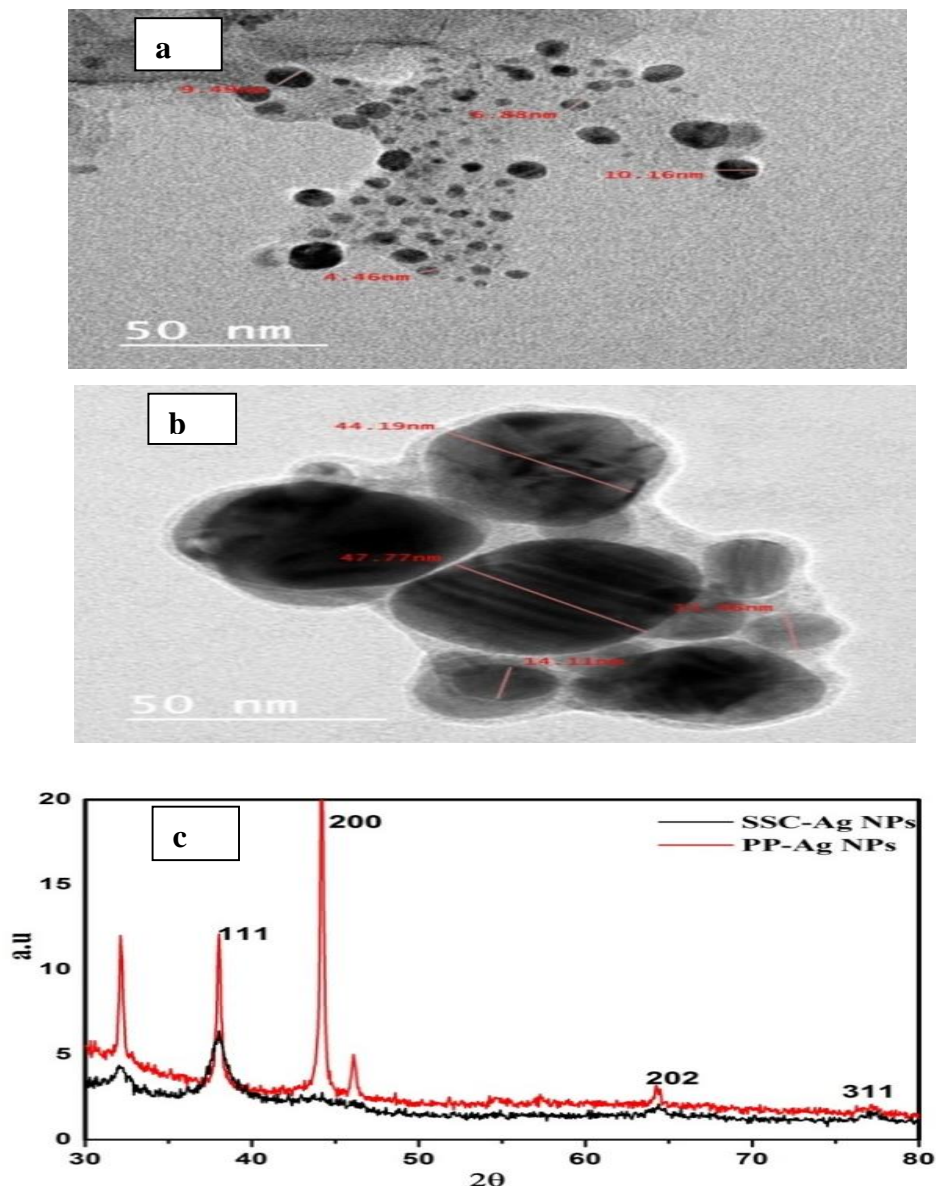


Fig.2: TEM micrograph of SSC-AgNPs (a) and pp-AgNPs (b). XRD pattern of SSC- AgNPs and PP- AgNPs(c).

3.5. Dynamic light scattering (DLS)

In the present study, the hydrodynamic size of SSC-AgNPs and PP-AgNPs was found to be 774.2 and 167.2 nm and the polydispersity index (PDI) was found to be 0.594 and 0.149 respectively as shown in Figure 3 (a & b). The low (PDI) value of PP-AgNPs indicated monodisperse sample while the high (PDI) value of SCC-AgNPs indicated the relatively polydisperse sample. Additionally, DLS studies showed that the zeta potential values of the SSC and PP AgNPs were, respectively, -9.79 and -24.22 mv Figure 3(c&d). This negative surface charge indicates that most of the capping molecules on the AgNPs' surface comprised up of negatively charged groups, which are also responsible for the degree of nanoparticles stability [25]. It was reported that, the proteins in the extract cap the synthesized AgNPs and impart a negative charge to the surface of nanoparticles [3]. Also, it was observed that the higher the zeta potential solution, the better the colloidal stability. Thus, the DLS studies in this investigation report the formation of monodispersed, non-agglomerated and stabilized PP-AgNPs compared to SSC-AgNPs.

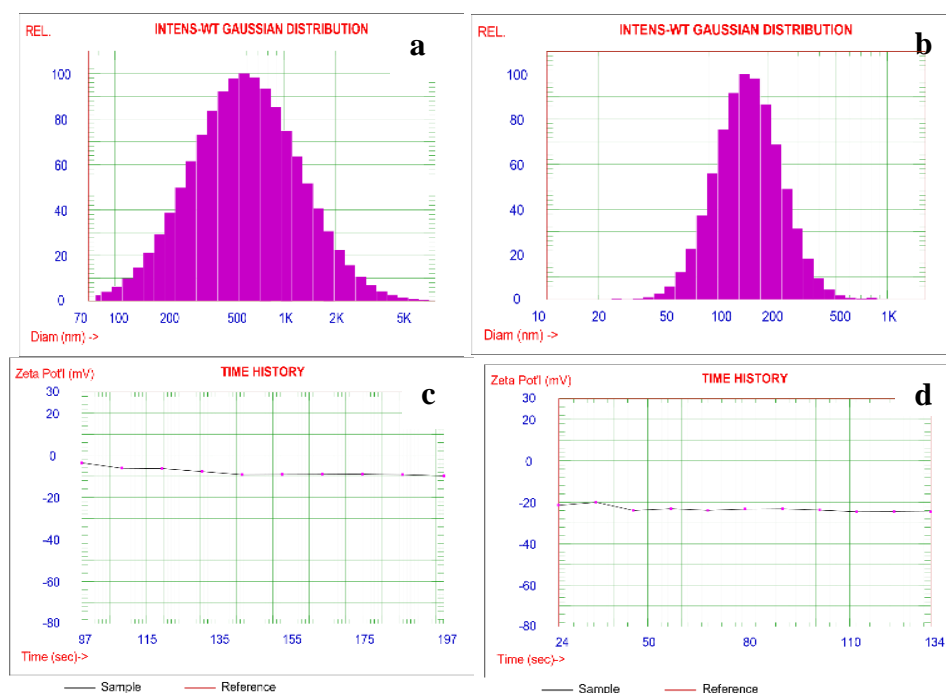


Fig.3: the hydrodynamic size (nm) and Zeta potential (mV) of SSC-AgNPs (a,c) and PP-AgNPs (b,d), respectively.

3.6. Hemolytic assay

Everything that enters the blood comes into contact with the red blood cells (RBCs). A hemolysis test was carried out through spectrophotometric measurement of hemoglobin release after exposure to varying concentrations (20000, 10000, 5000, 2000, 50 and 250) $\mu\text{g/mL}$ of SSC- AgNPs and PP-AgNPs. In order to evaluate the impact of AgNPs on erythrocytes. The hemolytic activity of SSC-AgNPs and PP- AgNPs exhibited dose-dependent hemolysis, in which PP-AgNPs was more potent than SSC-AgNPs at concentrations (20000, 10000, 5000, 2000, 500 and 250) $\mu\text{g/mL}$, SSC-AgNPs caused 60.05, 16.48, 8.48, 3.66, 1.40 and 1.10 % hemolysis while PP-AgNPs led to 92.6, 86.31, 83.35, 45.63, 6.17 and 3.94 % hemolysis as shown in Figure 4, hemolysis was 100% in deionized water. In comparison to positive control, nanoparticles synthesized with plant extract were generally less toxic to RBCs. Moreover, SSC-AgNPs and PP-AgNPs did not show any significant % hemolysis at concentration of 2000 and 250 $\mu\text{g/mL}$ respectively. This complies with ISO/TR 7406, which specifies a critical safe hemolytic ratio of 5% [26,27]. The results are consistent with previous reports. The blood compatibility of synthesized AgNPs using radish seeds with size in the range of 5–20 nm was compatible at concentration of 1000 $\mu\text{g/mL}$ (hemolysis % was 1.07)[25]. This result indicates that aggregation and moderate stability of smaller particle size nanoparticles led to the loss of a certain degree of their toxicity [6].

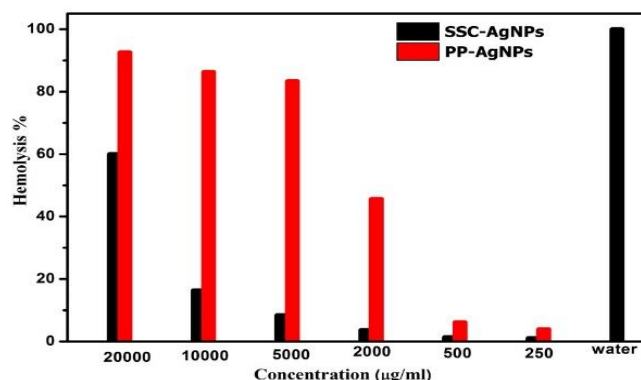


Fig.4: Percentage of hemolysis induced by SSC-AgNPs and PP-AgNPs respectively by using water as positive control.

3.7. Cytotoxic effect on human normal fibroblast (BJ1) and breast cancer (MCF7) cell line.

3.7.1. Cell viability assays:

(Cytotoxic activity of AgNPs) offer data on how cells respond to toxins, including their metabolism, survival, and death. In this study, the cytotoxic potential of SSC-AgNPs and PP-AgNPs against the BJ1 (normal Skin Fibroblast) human epithelial cell line was investigated. Using the MTT assay, the sample concentration ranges from 8000, 4000, 2000, 1000, 500, 250, 125 and 62.5 μ g/ml. The results that were obtained are shown in table (1). Both of SSC-AgNPs and PP-AgNPs exhibit cytotoxic effects on the normal human test cells at concentration of 2930 μ g/ml and 1341 μ g/ml, as shown by the results, although it is clear from the data that PP-AgNPs were more toxic than SSC-AgNPs by 54.2%. This is due to the difference in particles size and stability of them. Despite the smaller size and moderate stability of SSC-AgNPs lead to aggregation of its molecules reduced its toxic effect on the living cells on which it was tested [5,6] This result is comparable with its toxic effect on blood cell discussed above.

Table 1. Effect of SSC-AgNPs and PP-AgNPs on BJ1 (normal Skin fibroblast) and MCF7 [Human Caucasian breast adenocarcinoma]

Effect of tested samples on BJ1 (normal Skin fibroblast)			
Sample Code	LC ₅₀ (μ g/ml)	LC ₉₀ (μ g/ml)	Remarks
SSC-AgNPs	2930	5888	85.2% at 8000ppm
PP-AgNPs	1341	3668	100% at 8000ppm
DMSO	-----	-----	1% at 100ppm
Negative control	-----	-----	0 %
Effect of tested samples on MCF7 [Human Caucasian breast adenocarcinoma]			
Sample Code	LC ₅₀ (μ g/ml)	LC ₉₀ (μ g/ml)	Remarks
SSC-AgNPs	1787	3813	100% at 8000ppm
PP-AgNPs	1140	2610	100% at 8000ppm
DMSO	3% at 100ppm
Negative control	0%

Where:

IC₅₀: Lethal concentration of the sample which causes the death of 50% of cells in 48 hrs

IC₉₀: Lethal concentration of the sample which causes the death of 90% of cells in 48 hrs

Also, the impact of silver nanoparticles on the viability of MCF7 [Human Caucasian breast cancer] was investigated. Effectiveness and selective toxicity are the two most crucial criteria for cancer treatments [28,29]. The results of the MTT assay revealed that both SSC-AgNPs and PP-AgNPs reduced cancer cell viability at concentration of 1787 μ g/ml and 1140 μ g/ml respectively. Moreover, it showed that PP-AgNPs were more toxic than SSC-AgNPs by 36.2%. This finding suggests their remarkable efficiency in killing cancer cells is a result of their capacity to trigger apoptosis, which activates reactive oxygen species in these cancer cells, causing cell membrane degradation, oxidative stress, and apoptosis. This suggestion is consistent with the inferences of a previous report [30] the results from our study suggest remarkable efficiency of both prepared AgNPs in killing cancer cells at very low concentration compared to the concentration that exhibit cytotoxic effect on normal cell. Moreover, as indicated in table 1 and Figure.4, SSC-AgNPs at concentration of 2000 μ g/ml have no significant hemolysis % of red blood cell and less damaging effects on normal cells while it reduced cancer cell viability at concentration of 1787 μ g/ml. In contrast to PP-AgNPs, the concentration of 1140 μ g/ml that reduced cancer cell viability has highly significant hemolysis % of red blood cell and damaging effects on normal cells. Therefore, SSC -AgNPs are better suited for the treatment of cancer. A recent study reported less toxicity of the AgNPs produced from *Amigdalus spinosissima* against normal L929 cells [31]. Also, previous studies reported that AgNPs had no significant effects on normal cells [32].

3.8. The antimicrobial activity

In our study, the antimicrobial activity of SSC-AgNPs and PP-AgNPs against *Enterococcus faecalis*, *Staphylococcus aureus* and *Candida albicans* was evaluated by measuring inhibition zones. The inhibition zones for SSC- AgNPs and PP- AgNPs are shown in Figure 5(a,b&c) . The inhibition zone diameter for all the samples were measured and illustrated in table 2. The obtained results illustrated that both the prepared samples have clear antimicrobial effect on all the tested microorganisms. For SSC- AgNPs and PP- AgNPs, the inhibition zone diameters were 12, 13 & 17 mm and 21, 15.6 & 13.3 mm against *Enterococcus faecalis*, *Staphylococcus aureus* and *Candida albicans* respectively. From the data we noted that, SSC-AgNPs have higher antibacterial activity against *Staphylococcus aureus* than *Enterococcus faecalis* but less than the control whereas, PP- AgNPs have higher antibacterial activity against *Enterococcus faecalis* and also higher than the control by 25 %. By comparing the two prepared samples, PP- AgNPs were more efficient for *Enterococcus faecalis* and *Staphylococcus aureus* than SSC- AgNPs but SSC- AgNPs have higher antifungal activity against *Candida albicans* than PP- AgNPs.

Table 2. Antimicrobial activity of the SSC- AgNPs and PP- AgNPs samples by measuring zone of inhibition (mm) applying the well diffusion technique:-

Test bacteria	Code	SSC-AgNPs			Reference		PP-AgNPs			Reference	
	No. of trials	1	2	3	CN	MIZ	1	2	3	CN	MIZ
<i>Enterococcus faecalis</i>		12	12	12	19	36	20	21	22	16	Nil
<i>Staphylococcus aureus</i>		13	13	13	19	22	16	16	15	22	Nil
<i>Candida albicans</i>		17	17	17	Nil	18	13	14	13	Nil	14

Where: Nil means no antimicrobial activity and Reference, CN is Gentamicin mcg (standardized antibiotic disc) Bioanalyse and MCZ Miconazole 10 mcg (standard antifungal disc) Bioanalys.

The minimum inhibitory concentration values MIC were evaluated using Nutrient Broth medium applying Micro dilution broth method. The obtained results corresponded to those received in the agar-gel diffusion method were illustrated in table 3. From the illustrated data we deduced that the highest MICs of SSC Ag-NPs were reported in *Enterococcus faecalis* sample which equal to 93.75 µg /200.0 µL but *Staphylococcus aureus* and *Candida albicans* have lower MIC value 46.785 µg /200.0 µL. Where for PP- AgNPs, the lowest MICs were reported in *Enterococcus faecalis* is equal to 93.75 but equal to 187.5 for *Staphylococcus aureus* and *Candida albicans*. The OD reduction % was calculated from the obtained data by applying in equation (2) in the experimental part and illustrated in Figure 5(d). It was 53.02, 98.99 and 74.496 % for SSC- AgNPs and 85.877, 95.61 and 96.94 % reported for *Enterococcus faecalis*, *Staphylococcus aureus* and *Candida albicans* respectively by PP-AgNPs samples. By comparing the obtained results of MIC values for SSC- AgNPs and PP- AgNPs samples, we deduced that PP- AgNPs samples have more efficient antimicrobial properties than SSC- AgNPs samples. This may be due to the aggregation of SSC-AgNPs which reduce their antimicrobial impact [5, 6]. The smaller particles have more antibacterial effect compared to larger particles due to greater level of interaction [33&34]. Different physical factors affecting the potent mechanism of NPs depends on, shape, size and charge on molecules. Smaller AgNPs with the spherical or quasi-spherical format are more prone to silver release due to the large surface area [35]. With the help of capping agents, such dissolution behavior can be avoided by the surface modification of AgNPs [36]. Cell permeability could be altered by AgNPs smaller than 10 nm that can enter bacterial cells causing cell damage.

Table 3. The minimal inhibitory concentration (MIC) of the SSC- AgNPs and PP- AgNPs samples applying Micro dilution Broth assay: -

Test strain	O.D. of different concentrations of SSC-AgNPs							
Conc. µg /200.0 µL	1000	500	250	125	62.5	31.25	Blank	MIC µg /200.0 µL
<i>Enterococcus faecalis</i>	0.004	0.005	0.019	0.164	0.274	0.373	0.149	93.75
<i>Staphylococcus aureus</i>	0.004	0.008	0.014	0.059	0.099	0.202	0.149	46.875
<i>Candida albicans</i>	0.028	0.044	0.088	0.109	0.124	0.25	0.149	46.875
Test strain	O.D. of different concentrations of PP-AgNPs							
Conc. µg /200.0 µL	1000	500	250	125	62.5	31.25	Blank	MIC µg /200.0 µL
<i>Enterococcus faecalis</i>	0.194	0.219	0.239	0.267	0.331	0.414	0.262	93.75
<i>Staphylococcus aureus</i>	0.153	0.194	0.252	0.295	0.329	0.424	0.262	187.5
<i>Candida albicans</i>	0.188	0.242	0.257	0.283	0.312	0.35	0.262	187.5

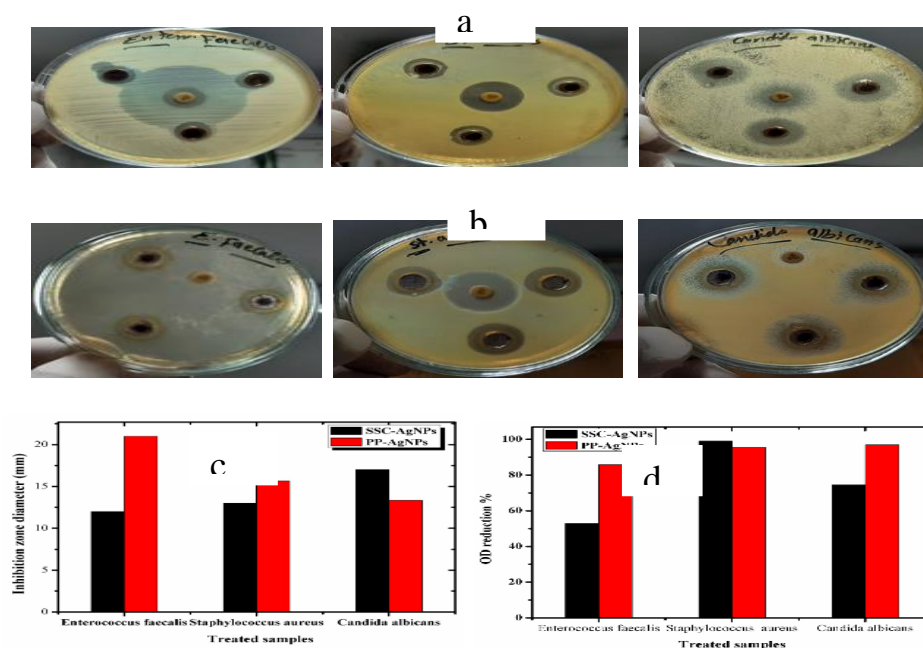


Fig.5: Inhibition zone images of SSC-AgNPs (a) and PP-AgNPs (b). Inhibition zone diameters (mm) (c) and OD reduction % (d) of SSC-AgNPs and PP-AgNPs against *Enterococcus faecalis*, *Staphylococcus aureus* and *Candida albicans*.

4. Conclusion

In our study AgNPs were successfully synthesized from a silver nitrate solution through a simple green route, using sunflower seed cake and pomegranate peel aqueous extract as a reducing as well as capping agent. Our results indicate that the aggregation behavior of AgNPs is mostly affected particle size and colloidal stability of AgNPs. It can also be assumed based on our findings that green synthesis of small sized and moderate stabilized AgNPs using biomolecules-poor oil seed cake extract might be suitable for biomedical applications compared to biomolecules-rich plant extract, since AgNPs with moderate stability undergo large-scale aggregation lose a certain degree of their blood and normal cell toxicity. However, they possessed good in vitro antimicrobial activity and anticancer activity in order to reliably use for therapeutic application such as drug delivery and cancer therapy.

5. Conflicts of interest

“There are no conflicts to declare”.

6. Formatting of funding sources

No funding.

7. References

- [1] N.V. Reddy, B.M. Satyanarayana, S. Sivasankar, D. Pragathi, K.V. Subbaiah, T. Vijaya, Eco-friendly synthesis of silver nanoparticles using leaf extract of *Flemingia wightiana*: spectral characterization, antioxidant and anticancer activity studies. *SN Appl. Sci.*, 2 (2020) 884. .
- [2] A.A. Alfuraydi, S. Devanesan, M. Al-Ansari, M. Al-Ansari, M.S. AlSalhi, A.J. Ranjitsingh, Eco-friendly green synthesis of silver nanoparticles from the sesame oil cake and its potential anticancer and antimicrobial activities, *journal of photochemistry and photobiology B: Biology*, 192 (2019) 83-89.
- [3] M. Govarthan, Y.S. Seo, K.J. Lee, I.B. Jung, H.J. Ju, J.S. Kim, M. Cho, S. Kamala-Kannan, Low-cost and eco-friendly synthesis of silver nanoparticles using coconut (*Cocos nucifera*) oil cake extract and its antibacterial activity *Artificial Cells, Nanomedicine, and Biotechnology*, 44 (2016) 1878-1882.
- [4] Y. Fu, J. Li, M. Almasi, Pomegranate peel extract - mediated synthesis of silver nanoparticle: evaluation of cytotoxicity, antioxidant and anti-esophageal cancer effect, *Chemistry Europe*, 8(15) (2023) e202204841.

- [5] A.A. Ashour, D. Raafat, H.M. El-Gowell, A.H. El-Kamel, Green synthesis of silver nanoparticles using cranberry powder aqueous extract: characterization and antimicrobial properties. *International Journal of Nanomedicine*, 10 (2015) 7207–7221.
- [6] P. Béteky, A. Rónavári, N. Igaz, B. Szerencsés, I.Y. Tóth, I. Pfeiffer, M. Kiricsi, Z. Kónya, Silver nanoparticles: aggregation behavior in biorelevant conditions and its impact on biological activity, *International Journal of Nanomedicine*, 14 (2019) 667–687.
- [7] A.S. Santhosh, S. Sandeep, H.M. Manukumar, B. Mahesh, N. Kumara Swamy, Green synthesis of silver nanoparticles using cow urine: Antimicrobial and blood biocompatibility studies. *JCIS Open*, 3 (2021) 100023.
- [8] R.A. Hamouda, M. Abd El-Mongy, K.F. Eid. Comparative Study between Two Red Algae for Biosynthesis Silver Nanoparticles Capping by SDS: Insights of Characterization and Antibacterial Activity. *Microbial pathogenesis*, 129 (2019) 224–232.
- [9] D. Mukundan, R. Mohankumar, R. Vasanthakumari, Comparative Study of Synthesized Silver and Gold Nanoparticles Using Leaves Extract of *Bauhinia Tomentosa* Linn and Their Anticancer Efficacy. *Bulletin of Materials Science*, 40 (2017) 335–344.
- [10] Y.Y. Loo, Y. Rukayadi, M.A.R. Nor-Khaizura, C.H. Kuan, B.W. Chieng, M. Nishibuchi, S. Radu, In Vitro Antimicrobial Activity of Green Synthesized Silver Nanoparticles Against Selected Gram-Negative Foodborne Pathogens. *Frontiers in microbiology*, 9 (2018) 1555.
- [11] T. Bruna, F. Maldonado-Bravo, P. Jara, N. Caro, Silver Nanoparticles and Their Antibacterial Applications, *International Journal of Molecular Sciences*, 22 (2021) 7202.
- [12] I.X. Yin, J. Zhang, I.S. Zhao, M.L. Mei, Q. Li, C.H. Chu, The Antibacterial Mechanism of Silver Nanoparticles and Its Application in Dentistry, *International journal of nanomedicine*, 9 (2020) 1555.
- [13] S. Elzey, V.H. Grassian, Agglomeration, isolation and dissolution of commercially manufactured silver nanoparticles in aqueous environments, *Journal of Nanoparticle Research*, 12(5) (2010) 1945–1958.
- [14] F.A. Bassyouni, S.M. Abu-Baker, K. Mahmoud, M. Moharam, S.S. El-Nakkady, M.A. Rehim, Synthesis and biological evaluation of some new triazolo[1,5- a]quinoline derivatives as anticancer and antimicrobial agents”. *RSC Advances*, 4 (2014) 24131-24141.
- [15] S.A. Awad, H.M. , Abd-Alla, H.I., Mahmoud, K.H., El-Toumy(2014): In vitro anti-nitrosative, antioxidant, and cytotoxicity activities of plant flavonoids: A comparative study, 23 (2014) 3298–3307
- [16] F. Abdelghaffar, R.A. Abdelghaffar, A.A. Arafa, M.M. Kamel, Functional Antibacterial Finishing of Woolen Fabrics Using Ultrasound Technology, *Fibers and Polymers*, 19(10) (2018) 2103-2111.
- [17] F.A. Mostafa, A.A. Abd El Aty, E.R. Hamed, B.M. Eid, Kinetic and anti-microbial studies on *Aspergillus terreus* culture filtrate and *Allium cepa* seeds extract and their potent applications, *Biocatalysis and Agricultural Biotechnology*, 5 (2016) 116-122.
- [18] Mc. Farland, The nephelometer: an instrument for estimating the number of bacteria in suspensions used for calculating the opsonic index and for vaccines, *Journal of the American Medical Association*, 49 (1907) 1176–1178.
- [19] A.A. El-anssary, G.F.A. Raoof, D.O. Saleh, H.M. El-Masry, Bioactivities, physicochemical parameters and GC/MS profiling of the fixed oil of *Cucumis melo* L. seeds: A focus on anti-inflammatory, immunomodulatory, and antimicrobial activities, *Journal of Herbmed Pharmacology*, 10(4) (2021) 476-485.
- [20] A.N. Elboraey, H.H. Abo-Almaged, A.A.E.R. El-Ashmawy, A.R. Abdou, A.R. Moussa, L.H. Emara, Biological and Mechanical Properties of Denture Base Material as a Vehicle for Novel Hydroxyapatite Nanoparticles Loaded with Drug, *Advanced Pharmaceutical Bulletin*, 11(1) (2021) 86.
- [21] S.A. Saquib, N.A. AlQahtani, I. Ahmad, M.A. Kader, SS Al Shahrani, E.A. Asiri, Evaluation and comparison of antibacterial efficacy of herbal extracts in combination with antibiotics on periodontal pathobionts: an in vitro microbiological study, *Antibiotics*, 8(3) (2019) 89.
- [22] M.A. Saied, K.A. Nour. Preparation and characterization of PMMA/ZnO nanocomposites for antistatic and biomedical applications. *Advances in Natural Sciences: Nanoscience and Nanotechnology*, 14(3) (2023) 035005.
- [23] A.P. Silveira, C.C. Bonatto, C.A. Lopes. Physicochemical characteristics and antibacterial effects of silver nanoparticles produced using the aqueous extract of *Ilex paraguariensis*. *material chemistry and physics*. 216 (2018) 476-484.
- [24] S. Negm, M. Moustafa, M. Sayed, S. Alamri, H. Alghamdii, A. Shati, M. Al-Khatani, S. Alrumman, T. Maghraby and H. Temerk. Antimicrobial activities of silver nanoparticles of extra virgin olive oil and sunflower oil against human pathogenic microbes *Pakistan Journal of Pharmaceutical Sciences*, 33(2020)2285-2291
- [25] S. Nayak, S.P. Sajankila, C.V. Rao, A.R. Hegde, S. Mutalik. Biogenic synthesis of silver nanoparticles using *Jatropha curcas* seed cake extract and characterization: evaluation of its antibacterial activity *Energy Sources, Part A: Recovery, Utilization, and Environmental Effects*, 43(2021)3415-3423.

- [26] S. Khare, R.K. Singh, O. Prakash . Green synthesis, characterization and biocompatibility evaluation of silver nanoparticles using radish seeds. *Results in Chemistry*, 4(2022).100447.
- [27] K. Jadhav, S. Deore, D. Dhamecha, R. H. Rajeshwari , S. Jagwani , S. Jalalpure , R. Bohara. .Phytosynthesis of Silver Nanoparticles: Characterization, Biocompatibility Studies, and Anticancer Activity. *ACS Biomater. Sci. Eng.* 4(3) 2018:892-899.
- [28] A. Eastman, R.P. Perez. New targets and challenges in the molecular therapeutics of cancer. *British journal of clinical pharmacology*, 62(1)(2006) 5-14.
- [29] I. Akbarzadeh, M. Shayan, M. Bourbour, M. Moghtaderi, H. Noorbazargan, ... & M. Tahriri,. Preparation, optimization and in-vitro evaluation of curcumin-loaded niosome@ calcium alginate nanocarrier as a new approach for breast cancer treatment. *Biology*, 10(3)(2021) 173.
- [30] N.E.A. El-Naggar, M.H. Hussein, A.A. El-Sawah. Bio-fabrication of silver nanoparticles by phycocyanin, characterization, in vitro anticancer activity against breast cancer cell line and in vivo cytotoxicity. *Scientific reports*, 7(1) (2017)10844.
- [31] S.B. Hariharan, HF Farahani, A.S. Rangwala, E. S. Oran& M. J. Gollner. Effects of natural and forced entrainment on PM emissions from fire whirls. *Environmental Science & Technology*, 56(6) (2022) 3480-3491.
- [32] S. Gurunathan, J.H. Park, J.W. Han, & J. H. Kim. Comparative assessment of the apoptotic potential of silver nanoparticles synthesized by *Bacillus tequilensis* and *Calocybe indica* in MDA-MB-231 human breast cancer cells: targeting p53 for anticancer therapy. *International journal of nanomedicine* 17 (2022)5207-5208.
- [33] Y. Dong, H. Zhu, Y. Shen, W. Zhang, L. Zhang. Antibacterial activity of silver nanoparticles of different particle size against *Vibrio Natriegens*, *PloS one*, 14 (2019) e0222322.
- [34] C. Baker, A. Pradhan, L. Pakstis, D.J. Pochan, S.I. Shah. Synthesis and antibacterial properties of silver nanoparticles. *Journal of nanoscience and nanotechnology*, 5(2005):244-249.
- [35] R. Shanmuganathan, D. MubarakAli, D. Prabakar, H. Muthukumar, N. Thajuddin, S.S. Kumar, A. Pugazhendhi. An Enhancement of Antimicrobial Efficacy of Biogenic and Ceftriaxone-Conjugated Silver Nanoparticles: Green Approach. *Environ. Sci. Pollut. Res.* 25(2018)10362–10370.
- [36] V.T. Noronha, A.J. Paula , G. Durán , A. Galembeck , K.Cogo-Müller , M. Franz-Montan , N. Durán .Silver Nanoparticles in Dentistry. *Environmental Science and Pollution Research*, 33(2017) 1110-1126.